Available online at www.sciencedirect.com
SCIENCE DIRECT®
Biochemical and Biophysical Research Communications 334 (2005) 183–192
BBRC
www.elsevier.com/locate/ybbrc

How actin crosslinking and bundling proteins cooperate to generate an enhanced cell mechanical response ☆

Yiider Tseng [a], Thomas P. Kole [a], Jerry S.H. Lee [a], Elena Fedorov [b], Steven C. Almo [b], Benjamin W. Schafer [c], Denis Wirtz [a,*]

[a] Department of Chemical and Biomolecular Engineering and Program in Molecular Biophysics, The Johns Hopkins University, Baltimore, MD 21218, USA
[b] Department of Biochemistry, Albert Einstein College of Medicine, Yeshiva University, Bronx, NY 1046, USA
[c] Department of Civil Engineering, The Johns Hopkins University, Baltimore, MD 21218, USA

Received 24 May 2005
Available online 24 June 2005

Abstract

Actin-crosslinking proteins organize actin filaments into dynamic and complex subcellular scaffolds that orchestrate important mechanical functions, including cell motility and adhesion. Recent mutation studies have shown that individual crosslinking proteins often play seemingly non-essential roles, leading to the hypothesis that they have considerable redundancy in function. We report live-cell, in vitro, and theoretical studies testing the mechanical role of the two ubiquitous actin-crosslinking proteins, α-actinin and fascin, which co-localize to stress fibers and the basis of filopodia. Using live-cell particle tracking microrheology, we show that the addition of α-actinin and fascin elicits a cell mechanical response that is significantly greater than that originated by α-actinin or fascin alone. These live-cell measurements are supported by quantitative rheological measurements with reconstituted actin filament networks containing pure proteins that show that α-actinin and fascin can work in concert to generate enhanced cell stiffness. Computational simulations using finite element modeling qualitatively reproduce and explain the functional synergy of α-actinin and fascin. These findings highlight the cooperative activity of fascin and α-actinin and provide a strong rationale that an evolutionary advantage might be conferred by the cooperative action of multiple actin-crosslinking proteins with overlapping but non-identical biochemical properties. Thus the combination of structural proteins with similar function can provide the cell with unique properties that are required for biologically optimal responses.

Keywords: Actin; Cytoskeleton; Cell mechanics; Multiple-particle tracking microrheology; Fascin; α-Actinin

Upon association with actin filaments, actin-crosslinking proteins promote the formation of entangled actin filament networks and bundles that provide mechanical elasticity to support various cellular activities [1,2], including membrane protrusions, cell motility, and cell adhesion, through the formation of specialized cyto-architectures, including stress fibers [3–5], dorsal arcs [6], concave or convex bundles [7,8], geodesic arrays [9–12], and loose meshworks [13–15]. The formation of these complex architectures seems to be dictated by the type of actin-crosslinking protein and protein stoichiometry controlled by the expression in actin and crosslinking proteins, the kinetics of actin polymerization, and the regulation of crosslinking activity. The modulation of actin-crosslinking proteins is critical during embryonic tissue development; for example, deficiency of α-actinin-3 leads to muscular dystrophy [16]. The expression levels of several actin-crosslinking proteins is also correlated with cell tumorigenicity [17].

☆ *Abbreviations:* MSD, mean squared displacement; MPTM, multiple-particle tracking microrheology.

* Corresponding author. Fax: +1 410 516 5510.
E-mail address: wirtz@jhu.edu (D. Wirtz).

0006-291X/$ - see front matter © 2005 Elsevier Inc. All rights reserved.
doi:10.1016/j.bbrc.2005.05.205

Smooth muscle α-actinin is a known transformation-sensitive marker in NIH3T3 and rat-2 cells [18]; in simian virus 40-transformed 3T3 cells, over-expression of α-actinin suppresses tumorigenicity [19]. Fascin expression also correlates with cell transformation and invasiveness [20]; for example, fascin is undetectable in normal epithelium, but is dramatically up-regulated in colorectal adenocarcinoma [21]. Together, these results suggest that the modulation of actin-crosslinking proteins plays a determinant role in cell function and, given the structural function of F-actin crosslinkers, in cell mechanics.

Over the past three decades, more than 23 different classes of proteins have been shown to crosslink F-actin [22]. Whether these crosslinking proteins with seemingly similar function have redundant or unique structural properties remains in dispute. The specialized subcellular localization of many F-actin crosslinkers suggest that each of these auxiliary proteins may play a unique role in orchestrating the dynamic organization of actin architectures that coordinate specific cellular activities. For instance, Arp2/3 complex is mainly localized to the cell periphery[23] and spectrin is exclusively localized to the inner surface of the plasma membrane. These F-actin crosslinkers can work in concert; for instance, using *Drosophila* as a model system, Tilney et al. [24,25] found that the two actin-crosslinking proteins fascin and forked play complementary roles in the formation of specific structures which modulate the morphology of bristles. However, several lines of evidence suggest that actin crosslinking proteins have redundant roles. For instance, actin crosslinkers often co-localize to the same subcellular organelles, e.g., α-actinin and fascin co-localize to stress fibers and the basis of filopodia along with several other F-actin crosslinking proteins. Moreover, several genetic studies have shown that individual cytoskeletal components are seemingly not essential, suggesting that there is considerable redundancy in function [26–29]. Whether the particularly large number of crosslinking proteins in the same cell reflects functional redundancy (to potentially enhance cell survival?) or that the combination of structural proteins of similar function provides the cell with unique properties for biologically optimal responses remains unknown.

Actin-crosslinking proteins interact with F-actin through bivalent actin-binding [30]. The proximal distance between two actin-binding sites of an actin-crosslinking protein seems to correlate with the ultrastructural properties of the actin filament network. Electron microscopy studies show that filamin, a v-shaped homodimer with the actin-binding sites located at the tips separated by a flexible molecular arm, crosslinks F-actin into a loose and mostly orthogonal network at low filamin/actin molar ratios and tight bundles at high molar ratios [31]. Similarly, α-actinin has a 40-nm spacer between its two actin-binding sites and crosslinks actin filaments into loose networks at low α-actinin/actin molar ratio and tight bundles at high molar ratios [32,33]. Fascin, a compact actin bundling protein that has two actin-binding sites within 12 nm (Almo, unpublished data), forms tightly packed parallel actin bundles at low fascin/actin molar ratios [34]. Together, these results suggest that the subcellular morphology of actin filament networks is determined partly by the structural properties of actin-crosslinking proteins.

Here, we report live-cell, in vitro, and theoretical studies testing the redundant/synergistic mechanical roles of two ubiquitous actin-crosslinking proteins, α-actinin and fascin. Using the method of multiple-particle tracking microrheology [35–40], we show that the addition of α-actinin and fascin in live cells elicits a synergistic mechanical response that is significantly greater than originated by α-actinin or fascin alone. Quantitative rheological measurements with reconstituted actin filament networks further support the hypothesis that α-actinin and fascin can work cooperatively to generate an enhanced mechanical response. Computational simulations using finite element modeling qualitatively reproduce and explain the mechanical synergy of α-actinin and fascin observed in live cells and in vitro.

Materials and methods

Protein purification. Actin was prepared from chicken skeletal muscle, gel-filtrated, and purified as described [33]. Mg^{2+}-actin filaments were generated by adding 1 volume of 10× KMEI (500 mM KCl, 10 mM $MgCl_2$, 10 mM EGTA, and 100 mM imidazole, pH 7.0) to 9 volumes of G-actin in buffer G (0.2 mM ATP, 0.5 mM DTT, 0.2 mM $CaCl_2$, 1 mM sodium azide, and 2 mM Tris–HCl, pH 8.0). α-Actinin was purified from chicken smooth muscle as described [41]; fascin was expressed in *Escherichia coli* and purified as described [34].

Mechanical rheometry in vitro. To measure the mechanical properties of F-actin solutions in vitro, a cone-and-plate, strain-controlled rheometer (ARES-100 Rheometrics, Piscataway, NJ) was employed as described [33]. G-Actin solutions were mixed with fascin, α-actinin or a mixture of fascin and α-actinin in a test tube; 10× KMEI was added to each solution, which was immediately loaded onto the lower plate of the rheometer. At steady state, oscillatory shear deformations of controlled frequency and amplitude were applied; the in-phase and out-of-phase components of the stress were then measured to compute viscoelastic moduli. Here, we report the elastic modulus G' and the phase angle $\delta = \tan^{-1}(G''/G')$, where G'' is the loss modulus, which characterizes viscous dissipation within sheared networks.

Cell culture and cell microinjection. Swiss 3T3 fibroblasts obtained from ATCC (Manassas, VA) were maintained at 37 °C in a humidified environment containing 5% CO_2 in Dulbecco's modified Eagle's medium (DMEM/F12) supplemented with 10% bovine calf serum (ATCC). Cells were microinjected with yellow-green, fluorescent, carboxylate-modified, 100 nm diameter nanospheres (Molecular Probes, Eugene, OR) using the Eppendorf Transjector 5246 (Brinkmann Instruments, Westbury, NY) following a method adapted from Beckerle [42]. After injection of probe nanospheres, cells were washed with Hanks' balanced salt solution and incubated overnight in serum-free medium.

Live-cell particle tracking microrheology. The trajectories of microinjected nanospheres imbedded in cytoplasm of cells were recorded using a SIT camera (VE-1000 Dage-MTI, Michigan City, IN) mounted on an inverted epifluorescence microscope equipped with a 100× oil-immersion lens (N.A. 1.3) (Nikon, Melville, NY) [43]. The coordinates of individual nanospheres, defined as the intensity-weighted centroid, were tracked with ≈5 nm resolution [44]; for each tested condition, 5–7 cells were probed and the trajectories of a total of 140 nanospheres were tracked. Movies of the movements of the fluctuating nanospheres were captured at a frame rate of 30 Hz for 20 s using the software Metaview (Universal Imaging, West Chester, PA) and analyzed using a custom routine incorporated to the software Metamorph (Universal Imaging) [45]. The cytoplasm is assumed to be *locally* isotropic, i.e., the measured trajectories faithfully represent 2D projections of 3D trajectories, which is reasonable given the Brownian nature of the probe movements. The mean squared displacement (MSD), $\langle \Delta r^2(\tau) \rangle$, of a nanosphere can be shown [46] to be proportional to the local compliance, $\Gamma(\tau) = 3/2(\pi a/k_B T)\langle \Delta r^2(\tau) \rangle$, of the specimen due to the small, local random force created by the fluctuating nanosphere. Here, k_B is the Boltzmann's constant, T is the absolute temperature, and a is the radius of the probe nanosphere. Local frequency-dependent elastic modulus $G'(\omega)$ and loss modulus $G''(\omega)$ were computed from individual MSD traces as described [47]. Neglecting inertial effects which only matter at MHz frequencies and assuming that the fluid surrounding the probe particles is incompressible, the viscoelastic spectrum $G(s)$, which is derived from a generalized Langevin equation for the motion of the nanosphere, is $G(s) = (2/3)k_B T/\pi as\langle \Delta r^2(s) \rangle$. Here, s is the Laplace frequency and $\langle \Delta r^2(s) \rangle$ is the unilateral Laplace transform of $\langle \Delta r^2(\tau) \rangle$. The elastic modulus $G'(\omega)$ and loss modulus $G''(\omega)$ are the real and imaginary parts, respectively, of the complex viscoelastic modulus $G_d(\omega)$, which is the projection of G(s) in Fourier space [47]. Shear viscosity was evaluated as the product of the plateau modulus at high frequencies and the relaxation, i.e., the inverse of the frequency at which G' and G'' were equal at low frequencies (see also [37–39]).

We have extensively tested MPTM on standard fluids and cytoskeleton networks in vitro. Quantitative agreement has been obtained between the viscoelastic moduli measured by conventional rheometry (using a strain-controlled rheometer) and those calculated from the MSD's of nanospheres imbedded in those standard fluids [44,47]. In particular, we verified that negatively charged, microinjected latex nanospheres did not undergo directed (motor-protein-driven) motion within cytoplasm [35,38]. Unlike those obtained with positively charged and endocytosed nanospheres, viscoelastic moduli calculated from negatively charged nanospheres were independent of their diameter [35]. These nanospheres showed extremely little non-specific binding to cell extracts as assessed by SDS–PAGE and a total protein assay [35]. We verified that cells were viable for at least 48 h after microinjection and that nanospheres were (somewhat evenly) split between daughter cells during cell division [35]. Moreover, microinjected nanospheres dispersed evenly throughout the cell, which permits a global characterization of the mechanics of a single cell (see Fig. 1A). These nanospheres are the same ones that we used previously to demonstrate the feasibility of particle tracking microrheology on standard fluids.

Fluorescence microscopy and actin filament organization in cells. Cell cultures were washed with PBS and fixed in 2.5% paraformaldehyde for 1 h. They were then washed with PBS and the cell membrane was pemeabilized by treatment with a 0.1% solution of Triton X-100 in PBS for 10 min. After rinsing with washing buffer (2% FCS), the cells were fixed in 10% FCS PBS and incubated in a 50 ng/ml solution of Alexa Fluor phalloidin (Molecular Probes) for 2 h. Cytoarchitecture of cells was visualized with a Nikon TE3000 inverted epifluorescence microscope, using a Nikon 100× Planfluor oil immersion objective (N.A. 1.3). Images were captured using a CCD camera (Hammamatsu, Bridgewater, NJ) controlled by the Metamorph/Metaview imaging software.

Confocal microscopy of reconstituted F-actin networks. To stain F-actin for fluorescence microscopy, 10 μl of 6.6 μM rhodamine phalloidin (Molecular Probes, Eugene, OR) in methanol was deposited on the microscopy chamber (PC20 CoverWell, Grace Biolab, Eugene, OR), and left to dry for 10 min [44]. G-actin samples suspended in a fluorescence buffer (1 mM $MgCl_2$, 50 mM KCl, 10 mM imidazole, pH 7.0, 100 mM DTT, 10 nM EDTA, 0.018 mg/ml catalase, 1 mg/ml glucose oxidase, and 3 mg/ml glucose) were placed immediately into the chamber well, mounted with a glass slide, and allowed to polymerize overnight at 4 °C. Samples were examined via a 100× oil-immersion objective (N.A. 1.3) with a Nikon PCM 2000 laser-scanning confocal system attached to a Nikon TE300 inverted microscope. Twenty optical sections collected, 0.5 μm apart, were combined to produce maximum projections of the actin gels using the software SimplePCI (Compix, Cranberry Township, PA).

Computer modeling. Calculations were performed using finite element analysis using the commercial software ABAQUS 5.8-16 (HKS, Providence, RI). Geometrically nonlinear static analysis (large deformations, no mass inertia) was conducted, where Newton's method was used for convergence of the equilibrium equations. Using Euler-Bernoulli beam elements, filaments and bundles were modeled as linear elastic fibers with YounG's modulus of 2.6 GPa and Poisson's ratio of 0.4 [48]. Perfect connection (i.e., no slip) was assumed between any two crossing fibers. A small axial pre-tension (1% of the total length) was assumed to engage the filament's axial stiffness. The ends of the filaments and bundles were pinned after the application of the pre-tension. The total out-of-plane loading was constant for all simulations and uniformly distributed on the fibers.

Results

Functional synergy of crosslinking protein α-actinin and bundling protein fascin in live cells

To test the mechanical function of individual F-actin crosslinkers and their possible synergistic function in live cells, we investigated the changes in the mechanical properties of Swiss 3T3 fibroblasts upon microinjection of α-actinin, fascin or mixtures of α-actinin and fascin. Live-cell viscoelastic properties were measured in situ via multiple-particle tracking microrheology (MPTM) (Fig. 1A). This method transforms measured Brownian displacements of nanospheres imbedded in cytoplasm into local viscous and elastic moduli. The time-dependent coordinates $[x(t), y(t)]$ (t, elapsed time) of the centroids of individual 50 nm-radius nanospheres were video-tracked with 5 nm spatial resolution and 33 ms temporal resolution (Figs. 1A and B), transformed into mean squared displacements (MSDs), $\langle \Delta r^2(\tau) \rangle = \langle [x(t\tau) - x(t)]^2 + [y(t\tau) - y(t)]^2 \rangle$ (τ, time scale or time lag) (not shown), and then transformed into compliance (i.e., deformability) profiles (Fig. 1C) and frequency-dependent viscoelastic moduli (not shown). The MSD of individual nanospheres is proportional to the local deformation (i.e., compliance) of the cytoplasm in response to the small local force created by the fluctuations of the probe nanosphere [46]. Details about MPTM can be found in [35,49]. These papers offer a thorough description of control experiments involving

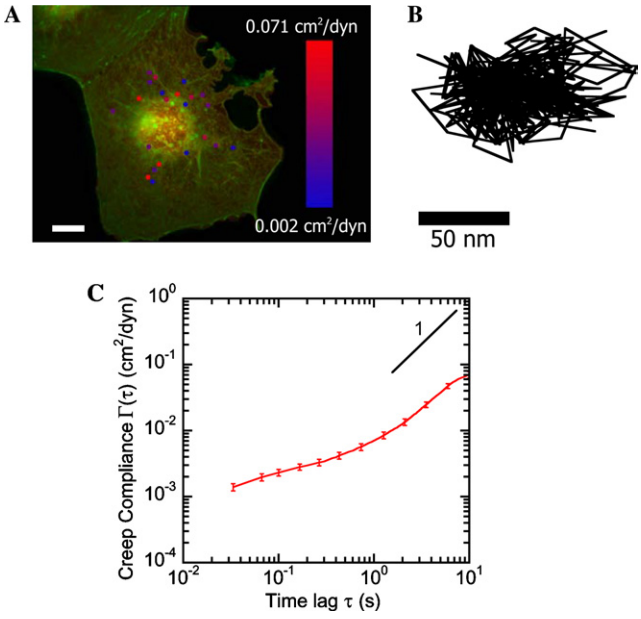

Fig. 1. Particle tracking microrheology of live fibroblasts. (A) Live-cell particle tracking microrheology: DIC micrograph of a cell plated on poly-L-lysine superimposed to a fluorescence micrograph of the trajectories of 0.1 μm-diameter PS nanospheres injected. The thermally excited motion of the nanospheres is monitored via multiple-particle video tracking. For illustration, the displacements are transformed into compliance and color coded according to their amplitude (soft, large compliance, stiff, small compliance measured at 20 s). The scaling bar represents 20 μm. (B) Typical trajectory of a nanosphere undergoing Brownian motion in a control cell. (C) Corresponding local compliance computed from the mean squared displacement (MSD).

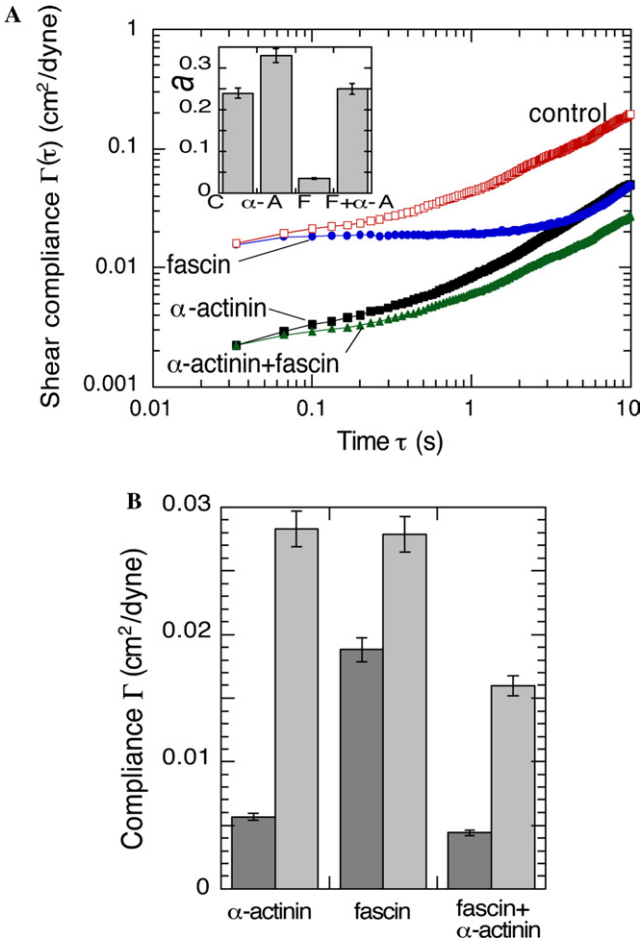

Fig. 2. Intracellular compliance of fibroblasts microinjected with the F-actin crosslinking/bundling proteins fascin, α-actinin, or both. (A) Mean shear compliance of the cytoplasm of either control cells or cells injected with purified α-actinin, fascin, or a 50/50 mixture of α-actinin and fascin. (Inset) Exponent a of the effective power-law increase of the elasticity versus frequency, $G' \sim \omega^a$, over the 1–100 rad/s frequency range. (B) Mean shear compliance evaluated at 0.5 s (left column) and 5.0 s (right column) of cells injected with α-actinin, fascin, or both.

nanospheres of different sizes and surface charges. In particular, specific and non-specific interactions between cytoplasmic cell extracts and the nanospheres were verified to be negligible. Measured mechanical properties were highly reproducible, exhibiting cell-to-cell variations as large or smaller than the differences between local moduli within a cell; mock injections of the microinjection buffer produced no measurable changes in cell mechanics (data not shown) [35]. Moreover, the motion of the nanospheres was verified to be purely Brownian, i.e., not directed (potentially) by motor proteins [50].

We investigated the effect of exogenous F-actin crosslinking and bundling proteins in serum-starved cells [39]. We found that serum-starved cells co-injected with α-actinin and fascin were significantly stiffer (i.e., less compliant) than α-actinin-injected cells, which in turn were stiffer than fascin-injected cells and control cells (Figs. 2A and B). This mechanical hierarchy suggests that crosslinking proteins α-actinin and fascin can work in concert to provide cells with enhanced mechanical strength. Compliance profiles displayed typically a shallow slope at short time scales and a steep slope at long time scales (Fig. 2A). Compliance profiles were transformed into frequency-dependent viscoelastic moduli as described [47] (see Materials and methods). Cells co-injected with α-actinin and fascin exhibited elastic moduli that were significantly higher than those of cells injected with fascin or α-actinin alone (Fig. 3A). These results indicate that α-actinin and fascin can function synergistically to provide cells with enhanced elasticity.

Microinjected fascin and α-actinin modulated not only the elasticity of the cytoskeleton but also its shear viscosity (Fig. 3B). The relative magnitude of viscosity to elasticity is evaluated by the phase angle, which determines whether a material behaves like a Hookean solid ($\delta = 0°$), a viscous liquid ($\delta = 90°$), or a viscoelastic element ($0° < \delta < 90°$) [51]. The ratio of the viscous modulus to elastic modulus of cells co-injected with fascin and α-actinin, which was similar to that of control cells, was intermediate between that of the cells injected with fascin alone, which were strongly solid-like, and the cells injected with α-actinin alone, which were more liquid-like (Fig. 3C and Table 1). Hence, cells co-injected with

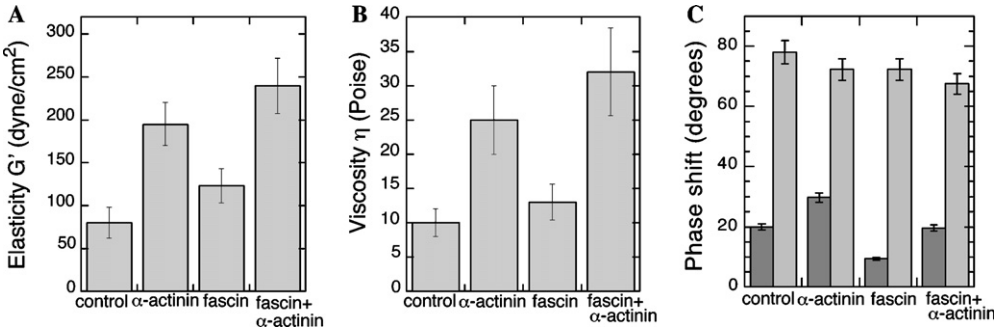

Fig. 3. Intracellular vicoelastic properties of fibroblasts microinjected with fascin, α-actinin, or both. (A) Mean elastic modulus evaluated at a frequency of $\omega = 1$ Hz (= 6.2 rad/s) of cells injected with α-actinin, fascin, or both (six cells, total probed nanospheres is 140). (B) Mean viscosity of either control cells or cells injected with α-actinin, fascin, or both. For comparison, the viscosity of water is 0.01 P. (C) Mean phase angle between elastic and loss moduli, $\delta = \tan^{-1}(G''/G')$, evaluated at 10 Hz (left column) and 0.1 Hz (right column) of either control cells or cells injected with α-actinin, fascin, or both. The phase angle of a viscous liquid is 90° and that of a Hookean solid is 0°.

Table 1
Viscoelastic moduli of Swiss 3T3 cells and cytoskeletal filament networks

In vitro	Elasticity (dyn/cm^2)[b]	Phase angle (deg)[b]	Frequency-dependence[c]	Live cell	Elasticity (dyn/cm^2)[d]	Phase angle (deg)[d]	Frequency-dependence[c]
F-actin[a]	12 ± 3	29 ± 5	++	Control cells	80 ± 20	25 ± 5	++
F-actin + α-actinin	440 ± 20	20 ± 3	+++	Cells + α-actinin	190 ± 30	29 ± 6	+++
F-actin + fascin	85 ± 8	12 ± 3	+	Cells + fascin	120 ± 25	9 ± 2	+
F-actin + fascin + α-actinin	990 ± 75	15 ± 2	++	Cells + fascin + α-actinin	240 ± 35	19 ± 4	++

[a] Actin concentration was 24 μM ≈ 1 mg/ml; α-actinin, fascin + α-actinin concentrations were 1.2 μM.
[b] Elasticity and phase angle in vitro were measured by applying an oscillatory deformation of 1 rad/s frequency and 1% strain amplitude.
[c] As measured by the frequency dependence of $G'(\omega)$ over the range 1–100 rad/s.
[d] Elasticity and phase angle in live cells were evaluated at 1 rad/s using MSD measurements as described in the text.

α-actinin and fascin are stiffer than cells injected with α-actinin and fascin separately and display an intermediate viscoelastic character, which is close to that displayed by control cells.

The local dynamic response of cytoplasm was assessed through the time-dependence of the compliance profiles and, equivalently, the frequency dependence of the elastic modulus. A strong frequency dependence of $G'(\omega)$ or strong time-dependence of the compliance profile indicates that the (small) stress created by the nanosphere's fluctuations relaxes and dissipates rapidly presumably due to rapid macromolecular motion in the vicinity of the probe nanospheres. Vice versa, weak frequency dependence of G' signifies that fluctuating stresses in the vicinity of the probe nanospheres are not rapidly dissipated. The time-dependence of the compliance in cells co-injected with both α-actinin and fascin was intermediate between that of α-actinin-injected cells and fascin-injected cells (Fig. 2A). The elasticity of cytoplasm was frequency-dependent at low frequencies and mostly independent of frequency at high frequencies, i.e., cells resist high rates of deformations effectively, but do not resist deformations that are applied slowly. Similarly, the frequency dependence of the elastic modulus indicated that cytoplasmic dynamics was greatest in α-actinin-injected cells and lowest in fascin-injected cells. Cells co-injected with both α-actinin and fascin exhibited an elasticity that had a frequency dependence, $G'(\omega) \sim \omega^a$, which was intermediate. Hence, the rate-dependent response of hybrid cells microinjected with both α-actinin and fascin is intermediate between the responses of α-actinin-injected cells and fascin-injected cells.

Functional synergy of α-actinin and fascin in vitro

To begin to understand the origin of the synergistic enhancement of cell stiffness by the actin crosslinking proteins α-actinin and fascin, we turned to F-actin networks reconstituted with pure proteins. The mechanical behavior of F-actin networks in the presence and absence of α-actinin and fascin was tested in vitro using rheometry, which measures viscoelastic moduli by computing the in- and out-of-phase components of the stress induced within the networks by applied oscillatory deformations [51]. To allow a more direct comparison of rheological measurements in vitro with MPTM measurements in live cells presented above, rheometric measurements were conducted at very small deformation amplitudes (=1%). Both MPTM and small-deformation rheology measure frequency-dependent moduli in the so-called linear regime for which moduli are

independent of the deformation amplitude [47]. Rheometric measurements therefore complement our previous measurements of reconstituted F-actin/α-actinin/fascin networks obtained at large deformation amplitudes [52,53]. In the absence of associated proteins, F-actin networks formed in vitro exhibited poor mechanical resilience and low elasticity (Fig. 3A and Table 1) [54]. As expected from previous work, α-actinin and fascin separately enhanced the stiffness of F-actin networks in vitro (Figs. 4A and B) [34]. However, F-actin networks containing both fascin and α-actinin were much stiffer than F-actin networks bundled/crosslinked by the same amount of α-actinin or fascin alone over a wide range of protein concentrations (Fig. 4B).

The behavior of actin filament networks was further examined by systematically varying the molar ratio of fascin to α-actinin, which exhibited a maximum in network stiffness between the minima displayed by pure F-actin/fascin and F-actin/α-actinin networks (Fig 4B). The elasticity of F-actin/α-actinin/fascin networks with a 1:1 molar ratio of fascin and α-actinin was between 30 and 200 times higher than that of pure F-actin, 5–14 times higher than that of F-actin/fascin networks and 1.5–3.5 times higher than that of F-actin/α-actinin networks (Fig. 4B).

Reconstituted actin filament networks crosslinked and bundled by α-actinin and fascin showed an intermediate viscoelastic character. Fascin decreased the phase angle of F-actin/α-actinin networks in vitro from ≈20° to 15°, i.e., when combined, fascin and α-actinin produced networks that are more liquid-like than fascin-crosslinked networks, but more solid-like (more elastic than viscous) than α-actinin-crosslinked networks (Table 1). These observations indicate that the cytoskeleton of living cells and F-actin/fascin/α-actinin networks assembled in vitro form structures that are similarly less dissipative than F-actin/α-actinin networks. The findings are of biological significance because a reduced dissipation in the actin cytoskeleton under mechanical stress allows, for instance, actin polymers to effectively transmit propulsive forces generated by actin assembly at the leading edge of motile cells [55]. These results show that α-actinin and fascin can synergistically enhance the stiffness of F-actin networks in vitro and endow F-actin networks with an intermediate viscoelastic character, in a manner similar to that observed in live cells.

The mobility of filaments in reconstituted F-actin networks in the presence of fascin and α-actinin was intermediate between that in the presence of α-actinin and fascin separately. Polymer mobility was assayed in vitro by applying (small) oscillatory deformations of increasing frequency and measuring the frequency dependence of the elastic modulus, $G'(\omega)$, in the linear regime of small deformations, the regime tested by the live-cell PTM assay. A high frequency-dependence for $G'(\omega)$ indicates that filaments are able to relax the stress presumably by diffusion [56]; in contrast, a weak frequency-dependence of the modulus indicates that individual filaments are highly constrained and do not readily move relative to the local filament network and therefore cannot relax stresses rapidly. This is the classical interpretation of frequency-dependent moduli profiles for polymer networks [56]. The dynamics of actin networks, measured by the frequency dependence of G', was greater in networks crosslinked by α-actinin than in networks crosslinked by fascin or networks crosslinked by both α-actinin and fascin (Fig. 4C and Table 1). These in vitro micromechanical measurements therefore qualitatively agree with the trends exhibited by the cytoskeleton of live cells, and demonstrate that crosslinking proteins can work in concert to enhance the

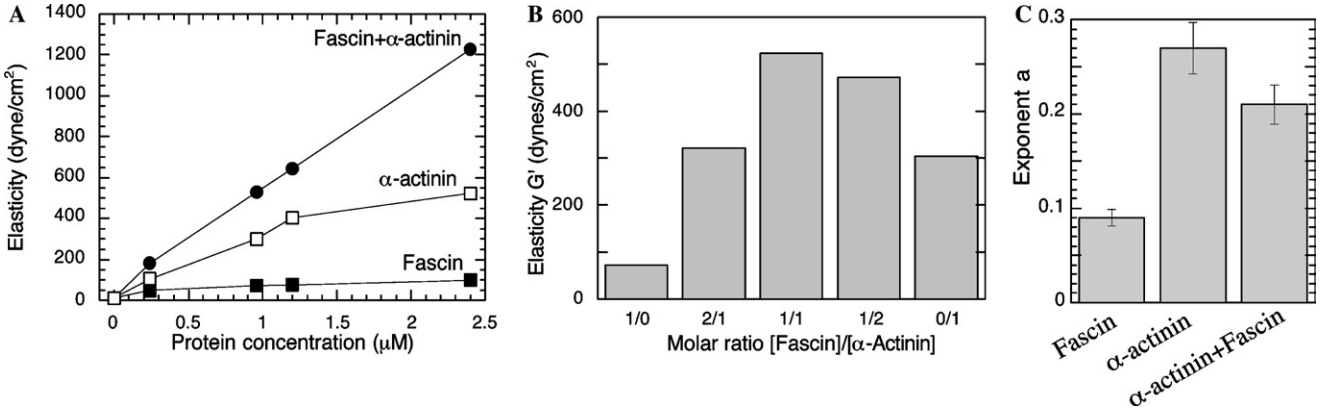

Fig. 4. Synergistic enhancement of the elasticity of reconstituted actin filament networks by combining α-actinin and fascin. (A) Elasticity of F-actin networks in the presence of increasing concentration of fascin (lower curve), α-actinin (intermediate curve), or both (upper curve). (B) Elasticity of F-actin/α-actinin/fascin networks for molar ratios of fascin-to-actinin ranging from 1:0 to 0:1. (C) Exponent a of the effective power-law increase of the elasticity versus frequency, $G' \sim \omega^a$, over the 1–100 rad/s frequency range. The elasticity and the phase angle of each network were measured by applying an oscillatory shear of 1 rad/s frequency and 1% amplitude. The total concentration of auxiliary proteins, [fascin] + [α-actinin], was constant and equal to 0.96 μM in (B,C). Actin concentration was 24 μM in all experiments.

mechanical response of F-actin networks and produced networks with intermediate dynamical properties.

Origin of mechanical synergy of crosslinking and bundling proteins: a computational model

We hypothesized that the origin of the mechanical synergy of α-actinin and fascin observed in live cells and in reconstituted actin filament networks was due to the mixed organization of actin filaments in bundles and crosslinked networks directed by these proteins. Fascin crosslinks actin filaments into highly ordered parallel bundles [57,58] readily; α-actinin crosslinks actin filaments into orthogonal arrays at low concentrations and into disordered bundles at high concentrations [59]. Fluorescence microscopy showed that cells co-injected with α-actinin and fascin displayed both F-actin bundles (also prominent in fascin-injected cells), and a dense orthogonal meshwork intertwined with loose bundles (also prominent in α-actinin-injected cells) (Figs. 5A and A″). Confocal microscopy of reconstituted actin filament networks in the presence of α-actinin and fascin showed straight bundles (predominantly present in F-actin/fascin networks) and a combination of orthogonal meshworks and loose bundles (predominantly present in F-actin/α-actinin networks) (Figs. 5B and B′).

To examine the hypothesis that bundles and crosslinked filaments act synergistically to enhance network stiffness, we utilized a highly simplified computer model of crosslinked cytoskeletal networks (see Materials and methods). The amount of material employed was constant and equal to 100×100 actin filaments for all simulated F-actin network architectures. These filaments were arranged symmetrically and orthogonally on a square area of $100\ \mu m^2$ supported around the outer edge. The filaments spanned the 100-μm distance as either individual filaments or as highly packed perfectly bonded 7 filament bundles (model results were the same for 19-filament bundles). As Fig. 6 demonstrates, the out-of-plane stiffness of the network of filaments and filament bundles is sensitive to the total number of individual filaments and filament-bundles. The stiffest network consists neither all filaments nor all bundles, rather a mixture of the two provides the optimum stiffness. This mechanical behavior corresponds grossly to the cases of F-actin + α-actinin, actin + α-actinin + fascin, and F-actin + fascin, respectively, which were considered in our in vitro and live-cell experiments in which combinations that induced some filament

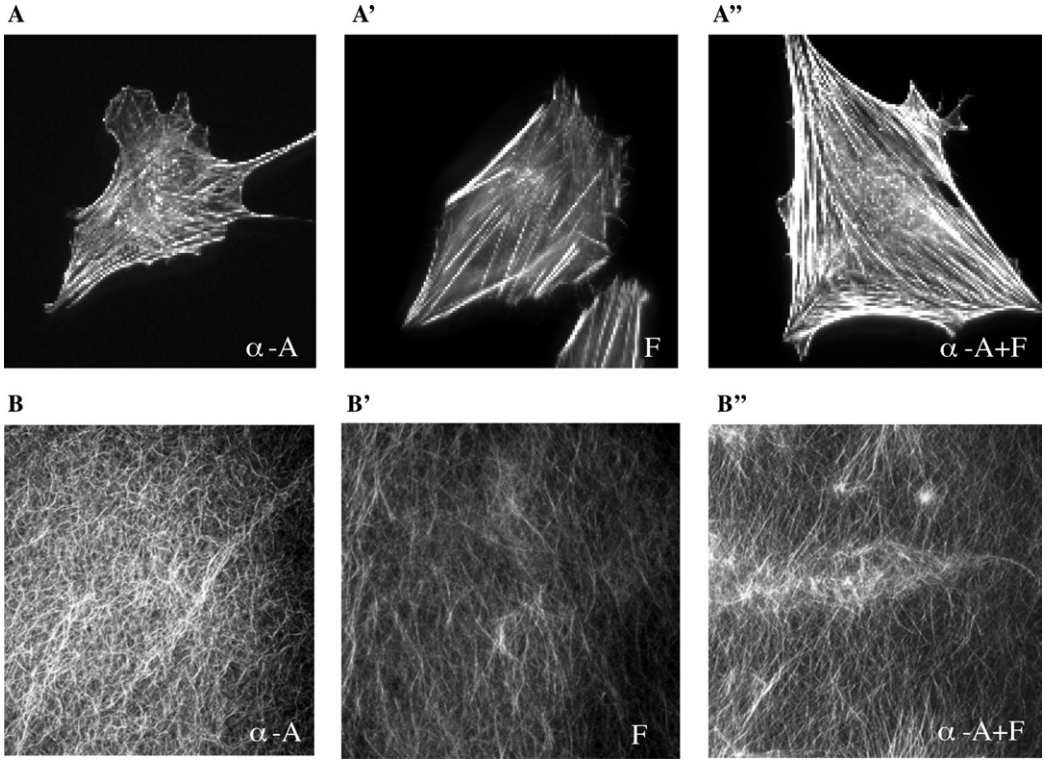

Fig. 5. Actin filament organization in cells microinjected with fascin, α-actinin, or both and corresponding organization of reconstituted F-actin networks. (A,A″) Fluorescence micrographs of cells injected with α-actinin (A), fascin (A′), or both (A″). The scaling bar in A represents 30 mm. (B,B″) Confocal micrographs of actin filament networks in the presence of α-actinin (B), fascin (B′), or both (B″). The scaling bar in B represents 30 μm.

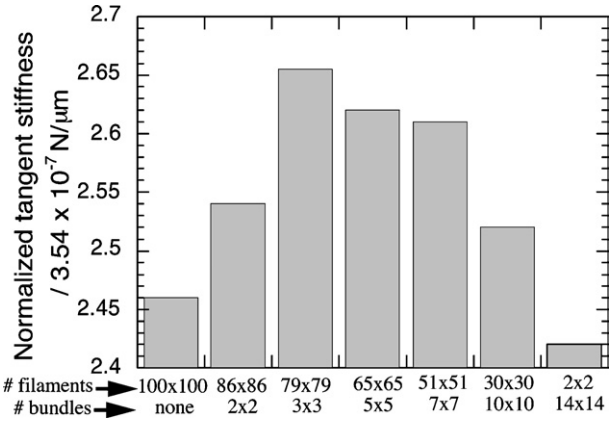

Fig. 6. Finite-element analysis of the mechanical response of a simplified model cytoskeletal ultrastructure containing a mixed arrangement of individual actin filaments and actin filament bundles. Bending stiffness measured at a deformation of 0.5 μm applied at the center of a symmetric, orthogonal array containing on each side either 100, 86, 79, 65, 51, 30, or 2 filaments and, respectively, either 0, 2, 3, 5, 7, 10, or 14 bundles. Each bundle contains seven filaments.

bundling and some filament crosslinking provided an optimum solution, as opposed to individual dopants. This simple model suggests that a mixed arrangement of crosslinked filaments and bundles displays an overall elasticity that is greater than in structures containing either mostly individual filaments or mostly filament bundles (Fig. 6).

Discussion

Live-cell microrheology has demonstrated that actin-crosslinking proteins can work cooperatively to enhance cell mechanical strength. Rheometric studies of reconstituted actin networks containing pure proteins and computer modeling suggest the origin of this synergistic effect. The superior mechanical behavior of mixed actin networking architectures that direct the assembly of both crosslinked filament networks and bundles are much stiffer than those containing only crosslinked orthogonal networks or only filament bundles. Our results in vitro are further supported by previous results with reconstituted actin networks which showed that, when combined, actin-crosslinking proteins can provide actin networks with superior resilience and feature enhanced strain-hardening under large deformations [52].

Motile cells extend a leading edge via the coordinated assembly of actin filaments and the organization of these filaments into resilient networks [2,60]. To prevent rearward movements of the filaments to drive the cell surface forward, polymerizing actin needs to be anchored to the substratum or crosslinked into stiff structures [60]. Our results suggest that α-actinin and fascin, which co-localize to the basis of cellular protrusions, could work synergistically to crosslink F-actin by exploiting the orthogonal crosslinking activity of α-actinin and the filament bundling activity of fascin. Previous work has shown, however, that F-actin-crosslinkers are capable of mediating the formation of orthogonal networks at low concentrations and bundles past a threshold concentration [59]. The molar ratio for bundle formation is ~1:150 for α-actinin and ~1:500 for fascin, respectively [34,59,61]. Therefore a high α-actinin concentration induces simultaneously filament bundling and crosslinking [59], and, according to our computational model, α-actinin alone could in principle generate high network elasticity and resilience. However, α-actinin produces F-actin structures that are less stiff and more dissipative than networks containing both α-actinin and fascin (Table 1). This is because α-actinin domain organization mediates the formation of loose and disorganized, as opposed to tightly packed, bundles. Similarly, fascin, an extremely effective bundling protein, crosslinks filaments into orthogonal networks at extremely low concentrations [34,62], but rather poorly as measured by the low elastic modulus of fascin-crosslinked networks. Hence, filaments crosslinked by fascin or α-actinin alone would be too dissipative and not sufficiently stiff to prevent filaments' rearward movements at the basis of cell protrusions. Our experimental and computational results suggest that it is much more effective for the actin cytoskeleton to combine bona fide actin-bundling proteins (e.g., fascin) and bona fide actin-crosslinking proteins (e.g., α-actinin).

The mechanical properties of tumor cells are expected to be dramatically different from normal cells as cancer cells feature a re-organized cytoskeleton and do not depend on adhesion to grow. A common feature of cancer cells is the loss of protein kinase C (PKC) modulation [63]. PKC phosphorylates fascin on Ser53 residue [64], which blocks the actin-crosslinking activity of fascin [65,66]. The PKC activity also affects its downstream signaling pathways, which includes PI3 kinase activity that would alter the PIP2-regulated actin-crosslinking activity of α-actinin [67]. Hence, in PKC modulation events, fascin and α-actinin activities are expected to be regulated simultaneously. Since α-actinin and fascin work synergistically, the regulation of these structural proteins is likely to mediate cytomechanical changes upon cancer cell transformation.

We believe that our observations are of considerable importance as they suggest the need to re-evaluate the much-invoked notion of functional redundancy among cytoskeletal regulatory proteins, in particular the actin-crosslinking proteins. Numerous genetic studies have shown that individual cytoskeletal components are not essential, leading the hypothesis that there is considerable redundancy in function [26–29]. The findings reported here highlight the synergistic activity of fascin and α-actinin and provide a strong rationale that an evolutionary advantage might be conferred by the

cooperative action of multiple actin-crosslinking proteins with overlapping but non-identical biochemical properties. Thus, the combination of structural proteins with seemingly similar function can provide the cell with unique properties that are required for biologically optimal responses.

Acknowledgments

These studies were supported in part by an NIH Grant AR42047 to S.C.A. and NASA Grant NAG9-1563 and NIH Grant GM075305 to D.W.

References

[1] S.R. Heidemann, S. Kaech, R.E. Buxbaum, A. Matus, Direct observations of the mechanical behaviors of the cytoskeleton in living fibroblasts, J. Cell Biol. 145 (1999) 109–122.
[2] S.R. Heidemann, D. Wirtz, Towards a regional approach to cell mechanics, Trends Cell Biol. 14 (2004) 160–166.
[3] T.E. Kreis, W. Birchmeier, Stress fiber sarcomeres of fibroblasts are contractile, Cell 22 (1980) 555–561.
[4] H.R. Byers, K. Fujiwara, Stress fibers in cells in situ: immunofluorescence visualization with antiactin, antimyosin, and anti-alpha-actinin, J. Cell Biol. 93 (1982) 804–811.
[5] Y.L. Wang, Reorganization of actin filament bundles in living fibroblasts, J. Cell Biol. 99 (1984) 1478–1485.
[6] J.P. Heath, Arcs: curved microfilament bundles beneath the dorsal surface of the leading lamellae of moving chick embryo fibroblasts, Cell Biol. Int. Rep. 5 (1981) 975–980.
[7] J.G. White, Arrangements of actin filaments in the cytoskeleton of human platelets, Am. J. Pathol. 117 (1984) 207–217.
[8] M.S. Zand, G. Albrecht-Buehler, What structures, besides adhesions, prevent spread cells from rounding up?, Cell Motil. Cytoskeleton 13 (1989) 195–211.
[9] R.A. Badley, A. Woods, L. Carruthers, D.A. Rees, Cytoskeleton changes in fibroblast adhesion and detachment, J. Cell Sci. 43 (1980) 379–390.
[10] J. Ciesielski-Treska, B. Guerold, D. Aunis, Immunofluorescence study on the organization of actin in astroglial cells in primary cultures, Neuroscience 7 (1982) 509–522.
[11] G.W. Ireland, E.J. Sanders, F.C. Voon, J. Wakely, The ultrastructure of polygonal networks in chick embryonic cells in vitro, Cell Biol. Int. Rep. 7 (1983) 679–688.
[12] Y. Mochizuki, K. Furukawa, T. Mitaka, T. Yokoi, T. Kodama, Polygonal networks, "geodomes," of adult rat hepatocytes in primary culture, Cell Biol. Int. Rep. 12 (1988) 1–7.
[13] L.G. Tilney, P. Detmers, Actin in erythrocyte ghosts and its association with spectrin. Evidence for a nonfilamentous form of these two molecules in situ, J. Cell Biol. 66 (1975) 508–520.
[14] I.K. Buckley, T.R. Raju, Form and distribution of actin and myosin in non-muscle cells: a study using cultured chick embryo fibroblasts, J. Microsc. 107 (1976) 129–149.
[15] J.A. Trotter, B.A. Foerder, J.M. Keller, Intracellular fibres in cultured cells: analysis by scanning and transmission electron microscopy and by SDS–polyacrylamide gel electrophoresis, J. Cell Sci. 31 (1978) 369–392.
[16] M. Vainzof, C.S. Costa, S.K. Marie, E.S. Moreira, U. Reed, M.R. Passos-Bueno, A.H. Beggs, M. Zatz, Deficiency of alpha-actinin-3 (ACTN3) occurs in different forms of muscular dystrophy, Neuropediatrics 28 (1997) 223–228.
[17] E. Button, C. Shapland, D. Lawson, Actin, its associated proteins and metastasis, Cell Motil. Cytoskeleton 30 (1995) 247–251.
[18] J. Leavitt, P. Gunning, L. Kedes, R. Jariwalla, Smooth muscle alpha-action is a transformation-sensitive marker for mouse NIH 3T3 and Rat-2 cells, Nature 316 (1985) 840–842.
[19] U. Gluck, D.J. Kwiatlowsky, A. Ben-Zeév, Suppression of tumorigenicity in Simian virus 40-transformed cells after transfection with vinculin cDNA, Proc. Natl. Acad. Sci. USA 90 (1993) 383–387.
[20] N. Kureishy, V. Sapountzi, S. Prag, N. Anilkumar, J.C. Adams, Fascins, and their roles in cell structure and function, Bioessays 24 (2002) 350–361.
[21] A.U. Jawhari, A. Buda, M. Jenkins, K. Shehzad, C. Sarraf, M. Noda, M.J. Farthing, M. Pignatelli, J.C. Adams, Fascin, an actin-bundling protein, modulates colonic epithelial cell invasiveness and differentiation in vitro, Am. J. Pathol. 162 (2003) 69–80.
[22] T. Kreis, R. Vale, Guidebook to the Cytoskeletal and Motor Proteins, Oxford University Press, Oxford, 1999.
[23] Y. Tseng, D. Wirtz, Dendritic branching and homogenization of actin networks mediated by Arp2/3 complex, Phys. Rev. Lett. 93 (2004) 258104.
[24] L.G. Tilney, M.S. Tilney, G.M. Guild, F-actin bundles in *Drosophila* bristles. I. Two filament cross-links are involved in bundling, J. Cell Biol. 130 (1995) 629–638.
[25] L.G. Tilney, P.S. Connelly, K.A. Vranich, M.K. Shaw, G.M. Guild, Why are two different cross-linkers necessary for actin bundle formation in vivo and what does each cross-link contribute?, J. Cell Biol. 143 (1998) 121–133.
[26] K. Cant, B.A. Knowles, S. Mahajan-Miklos, M. Heintzelman, L. Cooley, *Drosophila* fascin mutants are rescued by overexpression of the villin-like protein, quail, J. Cell Sci. 111 (1998) 213–221.
[27] D.E. Ingber, D. Prusty, Z. Sun, H. Betensky, N. Wang, Cell shape, cytoskeletal mechanics, and cell cycle control in angiogenesis, J. Biomech. 28 (1995) 1471–1484.
[28] S.M. Thomas, P. Soriano, A. Imamoto, Specific and redundant roles of Src and Fyn in organizing the cytoskeleton, Nature 376 (1995) 267–271.
[29] F. Rivero, R. Furukawa, M. Fechheimer, A.A. Noegel, Three actin cross-linking proteins, the 34 kDa actin-bundling protein, alpha-actinin and gelation factor (ABP-120), have both unique and redundant roles in the growth and development of *Dictyostelium*, J. Cell Sci. 112 (1999) 2737–2751.
[30] Y.A. Puius, N.M. Mahoney, S.C. Almo, The modular structure of actin-regulatory proteins, Curr. Opin. Cell Biol. 10 (1998) 23–34.
[31] Y. Tseng, K.M. An, O. Esue, D. Wirtz, The bimodal role of filamin in controlling the architecture and mechanics of F-actin networks, J. Biol. Chem. 279 (2004) 1819–1826.
[32] Y. Tseng, D. Wirtz, Mechanics and multiple-particle tracking microhetrogeneity of alpha-actinin-cross-linked actin filament networks., Biophys. J. 81 (2001) 1643–1656.
[33] J. Xu, D. Wirtz, T.D. Pollard, Dynamic cross-linking by α-actinin determines the mechanical properties of actin filament networks, J. Biol. Chem. 273 (1998) 9570–9576.
[34] Y. Tseng, E. Fedorov, J.M. McCaffery, S.C. Almo, D. Wirtz, Micromechanics and microstructure of actin filament networks in the presence of the actin-bundling protein human fascin: a comparison with α-actinin, J. Mol. Biol. 310 (2001) 351–366.
[35] Y. Tseng, T.P. Kole, D. Wirtz, Micromechanical mapping of live cells by multiple-particle-tracking microrheology, Biophys. J. 83 (2002) 3162–3176.
[36] Y. Tseng, J.S. Lee, T.P. Kole, I. Jiang, D. Wirtz, Micro-organization and visco-elasticity of the interphase nucleus revealed by particle nanotracking, J. Cell Sci. 117 (2004) 2159–2167.
[37] T.P. Kole, Y. Tseng, I. Jiang, J.L. Katz, D. Wirtz, Intracellular mechanics of migrating fibroblasts, Mol. Biol. Cell 16 (2005) 328–338.

[38] T.P. Kole, Y. Tseng, D. Wirtz, Intracellular microrheology as a tool for the measurement of the local mechanical properties of live cells, Methods Cell Biol. 78 (2004) 45–64.
[39] T.P. Kole, Y. Tseng, L. Huang, J.L. Katz, D. Wirtz, Rho kinase regulates the micromechanical response of adherent cells to Rho activation, Mol. Biol. Cell 15 (2004) 3475–3484.
[40] S.L. Gupton, K.L. Anderson, T.P. Kole, R.S. Fischer, A. Ponti, S.E. Hitchcock-DeGregori, G. Danuse, V.M. Fowler, D. Wirtz, D. Hanein, C.M. Waterman-Storer, Cell migration without a lamellipodium: translation of actin dynamics into cell movement mediated by tropomyosin, J. Cell Biol. 168 (2005) 619–631.
[41] S.W. Craig, C.L. Lancashire, J.A. Cooper, Preparation of smooth muscle alpha-actinin, Methods Enzymol. 85 (1982) 316–321.
[42] M.C. Beckerle, Fluorescent polystyrene beads exhibit saltatory motion in tissue-culture cells, J. Cell Biol. 98 (1984) 2126–2132.
[43] P. Leduc, C. Haber, G. Bao, D. Wirtz, Dynamics of individual flexible polymers in a shear flow, Nature 399 (1999) 564–566.
[44] J. Apgar, Y. Tseng, E. Federov, M.B. Herwig, S.C. Almo, D. Wirtz, Multiple-particle tracking measurements of heterogeneities in solutions of actin filaments and actin bundles, Biophys. J. 79 (2000) 1095–1106.
[45] Y. Tseng, K.M. An, D. Wirtz, Microheterogeneity controls the rate of gelation of actin filament networks, J. Biol. Chem. 277 (2002) 18143–18150.
[46] J. Xu, V. Viasnoff, D. Wirtz, Compliance of actin filament networks measured by particle-tracking microrheology and diffusing wave spectroscopy, Rheologica Acta 37 (1998) 387–398.
[47] T.G. Mason, K. Ganesan, J.V. van Zanten, D. Wirtz, S.C. Kuo, Particle-tracking microrheology of complex fluids, Phys. Rev. Lett. 79 (1997) 3282–3285.
[48] H. Kojima, A. Ishijima, T. Yanagida, Direct measurement of stiffness of single actin filaments with and without tropomyosin by in vitro nanomanipulation, Proc. Natl Acad. Sci. USA 91 (1994) 12962–12966.
[49] P. Panorchan, Y. Tseng, D. Wirtz, Structure–function relationship of biological gels revealed by multiple particle tracking and differential interference contrast microscopy: the case of human lamin networks, Phys. Rev. E 70 (2004) 041906.
[50] H.S. Jung, D. Wirtz, J. Hanes, Real-time intracellular tracking of non-viral gene carriers, Proc. Natl Acad. Sci. USA 100 (2003) 3878–3882.
[51] P.A. Coulombe, O. Bousquet, L. Ma, S. Yamada, D. Wirtz, The 'ins' and 'outs' of intermediate filament organization, Trends Cell Biol. 10 (2000) 420–428.
[52] Y. Tseng, B.W. Schafer, S.C. Almo, D. Wirtz, Functional synergy of actin filament crosslinking proteins, J. Biol. Chem. 277 (2002) 25609–25616.
[53] J. Xu, Y. Tseng, D. Wirtz, Strain-hardening of actin filament networks—regulation by the dynamic crosslinking protein α-actinin, J. Biol. Chem. 275 (2000) 35886–35892.
[54] M. Sato, W.H. Schwarz, T.D. Pollard, Dependence of the mechanical properties of actinα-actinin gels on deformation rate, Nature 325 (1987) 828–830.
[55] G.G. Borisy, T.M. Svitkina, Actin machinery: pushing the envelope, Curr. Opin. Cell Biol. 12 (2000) 104–112.
[56] P.-G. de Gennes, Scaling concepts in polymer physics, Cornell University Press, Ithaca, 1991.
[57] J.J. Otto, R.E. Kane, J. Bryan, Formation of filopodia in coelomocytes: localization of fascin, a 58,000 dalton actin cross-linking protein, Cell 17 (1979) 285–293.
[58] S. Yamashiro-Matsumura, F. Matsumura, Intracellular localization of the 55-kD actin-bundling protein in cultured cells: spatial relationships with actin, alpha-actinin, tropomyosin, and fimbrin, J. Cell Biol. 103 (1986) 631–640.
[59] D. Wachsstock, W.H. Schwarz, T.D. Pollard, Affinity of α-actinin for actin determines the structure and mechanical properties of actin filament gels, Biophys. J. 65 (1993) 205–214.
[60] T.D. Pollard, G.G. Borisy, Cellular motility driven by assembly and disassembly of actin filaments, Cell 112 (2003) 453–465.
[61] D.L. Stokes, D.J. DeRosier, Growth conditions control the size and order of actin bundles in vitro, Biophys. J. 59 (1991) 456–465.
[62] D.J. DeRosier, R. Censullo, Structure of F-actin needles from extracts of sea-urchin oocytes, J. Mol. Biol. 146 (1981) 77–99.
[63] I.H. Gelman, The role of SSeCKS/gravin/AKAP12 scaffolding proteins in the spaciotemporal control of signaling pathways in oncogenesis and development, Front. Biosci. 7 (2002) d1782–1797.
[64] S. Ono, Y. Yamakita, S. Yamashiro, P.T. Matsudaira, J.R. Gnarra, T. Obinata, F. Matsumura, Identification of an actin binding region and a protein kinase C phosphorylation site on human fascin, J. Biol. Chem. 272 (1997) 2527–2533.
[65] J.C. Adams, J.D. Clelland, G.D. Collett, F. Matsumura, S. Yamashiro, L. Zhang, Cell–matrix adhesions differentially regulate fascin phosphorylation, Mol. Biol. Cell 10 (1999) 4177–4190.
[66] Y. Yamakita, S. Ono, F. Matsumura, S. Yamashiro, Phosphorylation of human fascin inhibits its actin binding and bundling activities, J. Biol. Chem. 271 (1996) 12632–12638.
[67] K. Fukami, K. Furuhashi, M. Inagaki, T. Endo, S. Hatano, T. Takenawa, Requirement of phosphatidylinositol 4,5-bisphosphate for alpha-actinin function, Nature 359 (1992) 150–152.